10. N. Stahl *et al.*, *ibid.* **263**, 92 (1994).
11. J. Schlessinger and A. Ullrich, *Neuron* **9**, 383 (1992).
12. L. Velazquez, M. Fellous, G. R. Stark, S. Pellegrini, *Cell* **70**, 313 (1992).
13. D. Watling *et al.*, *Nature* **366**, 166 (1993).
14. M. Muller *et al.*, *ibid.*, p. 129.
15. N. Stahl, T. Boulton, G. D. Yancopoulos, unpublished data.
16. Z. Zhong, Z. Wen, J. E. Darnell, *Science* **264**, 95 (1994).
17. U. M. Wegenka *et al.*, *Mol. Cell. Biol.* **14**, 3186 (1994).
18. S. Akira *et al.*, *Cell* **77**, 63 (1994).
19. O. Silvennoinen, J. N. Ihle, J. Schlessinger, D. E. Levy, *Nature* **366**, 583 (1993).
20. T. G. Boulton, N. Stahl, G. D. Yancopoulos, *J. Biol. Chem.* **269**, 11648 (1994).
21. A. C. Greenlund, M. A. Farrar, B. L. Viviano, R. D. Schreiber, *EMBO J.* **13**, 1591 (1994).
22. C. A. Koch, D. Anderson, M. F. Moran, C. Ellis, T. Pawson, *Science* **252**, 668 (1991).
23. W. Li *et al.*, *Mol. Cell. Biol.* **14**, 509 (1994).
24. A. M. Bennet, T. L. Tang, S. Sugimoto, C. T. Walsh, B. G. Neel, *Proc. Natl. Acad. Sci. U.S.A.* **91**, 7335 (1994).
25. The EG series of chimeric receptors contained amino acids 1 to 645 of EGFR fused to the following portions of gp130. EG: 620 to 918; $EGDY_{4-5}$: 620 to 904; $EGDY_{3-5}$: 620 to 813; $EGDY_{2-5}$: 620 to 766; $EGDY_{1-5}$: 620 to 758. The EL-based chimeric receptors contained amino acids 1 to 645 of EGFR fused to the following portions of LIFR. EL: 834 to 1097; $ELDY_5$: 834 to 1027; $ELDY_{4-5}$: 834 to 1000; $ELDY_{3-5}$: 834 to 980; $ELDY_{1-5}$: 834 to 948. The TG chimeric receptors contained amino acids 1 to 458 of TrkC fused to amino acids 644 to 918 of gp130. TG(Y_1F) and TG(Y_2F) contain phenylalanine substituted for tyrosines 759 or 767, respectively. The receptor construct EGt corresponds exactly to the construct $EGDY_{1-5}$, whereas TGt contained amino acids 1 to 458 of TrkC fused to amino acids 644 to 758 of gp130.
26. H. Baumann *et al.*, *Mol. Cell. Biol.* **14**, 138 (1994).
27. Although the experiments depicted here demonstrate that PTP1D and Stat3 become inducibly associated with the anti-phosphotyrosine–precipitated protein fraction, separate experiments in which PTP1D and Stat3 were first precipitated with specific antibodies and then blotted with antibodies to phosphotyrosine confirmed that they were inducibly tyrosine phosphorylated in all cases.
28. R. D. Case *et al.*, *J. Biol. Chem.* **269**, 10467 (1994).
29. Z. Songyang *et al.*, *Cell* **72**, 767 (1993).
30. K. Shuai *et al.*, *ibid.* **76**, 821 (1994).
31. M. Narazaki *et al.*, *Proc. Natl. Acad. Sci. U.S.A.* **91**, 2285 (1994).
32. M. Murakami *et al.*, *ibid.* **88**, 11349 (1991).
33. M. Hatakeyama *et al.*, *Science* **252**, 1523 (1991).
34. M. H. Heim, I. M. Kerr, G. R. Stark, J. E. Darnell Jr., *ibid.* **267**, 1347 (1995).
35. D. M. Valenzuela *et al.*, *Neuron* **10**, 963 (1993).
36. We thank L. Schleifer and the entire Regeneron Discovery group for support; P. Jones and J. McClain for help with constructs; D. Valenzuela, J. Griffiths, and M. Gisser for molecular biology support; L. Defeo for cell culture; and C. Murphy for photography.

31 August 1994; accepted 20 December 1994

A p53-Dependent Mouse Spindle Checkpoint

Shawn M. Cross, Carissa A. Sanchez, Catherine A. Morgan, Melana K. Schimke, Stig Ramel, Rejean L. Idzerda, Wendy H. Raskind, Brian J. Reid*

Cell cycle checkpoints enhance genetic fidelity by causing arrest at specific stages of the cell cycle when previous events have not been completed. The tumor suppressor p53 has been implicated in a G_1 checkpoint. To investigate whether p53 also participates in a mitotic checkpoint, cultured fibroblasts from p53-deficient mouse embryos were exposed to spindle inhibitors. The fibroblasts underwent multiple rounds of DNA synthesis without completing chromosome segregation, thus forming tetraploid and octaploid cells. Deficiency of p53 was also associated with the development of tetraploidy in vivo. These results suggest that murine p53 is a component of a spindle checkpoint that ensures the maintenance of diploidy.

Genetic fidelity is achieved by the coordinated activity of genes and proteins that participate in DNA replication and chromosome segregation, cell cycle checkpoint controls, and repair pathways (*1*, *2*). In general, the onset of each stage of the cell cycle is dependent on successful completion of previous cell cycle events, and these dependencies are maintained by checkpoints (*2*). In the yeast *Saccharomyces cerevisiae*, several genes have been identified as components of a checkpoint that responds to spindle aberrations by causing cells to arrest in mitosis (*3*). Mutations in these genes can relieve the normal dependency of DNA synthesis on the completion of mitosis, permitting premature rounds of DNA synthesis in the presence of inhibitors that normally cause mitotic arrest, thereby leading to polyploidy. A similar checkpoint has been described in mammalian cells, but the genes that control it have not yet been identified.

The tumor suppressor p53 can be inactivated by allelic loss and mutation (*4*) and by interaction with viral oncoproteins, including SV40 T antigen (*5*). A p53-dependent G_1 checkpoint can prevent gene amplification by causing G_1 arrest after exposure to DNA damaging agents (*6*, *7*). However, the results of several studies suggest that p53 may be required for the maintenance of diploidy because loss or inactivation of p53 can be associated with tetraploidy or aneuploidy (*7*–*12*).

To investigate whether p53 participates in a mitotic checkpoint, we assessed the ability of fibroblasts from p53-deficient ($p53^{-/-}$) mouse embryos to arrest after exposure to spindle inhibitors in vitro. Wild-type ($p53^{+/+}$) mouse embryonic fibroblasts (MEFs) that were exposed to nocodazole or colcemid for 22 hours accumulated with a 4N DNA content and only a minority of cells reentered the S phase prematurely (Fig. 1, C and E). In contrast, $p53^{-/-}$ MEFs continued cell cycle progression after treatment with nocodazole or colcemid, forming cycling tetraploid and octaploid cell populations (Fig. 1, D and F).

To determine the fraction of $p53^{-/-}$ MEFs that escaped the spindle checkpoint and became polyploid, we investigated the proportion of cells that developed DNA contents greater than 4N (tetraploid S phase, octaploid) and 8N (octaploid S phase, greater ploidies) after 22 and 44 hours of exposure to each inhibitor. DNA contents greater than 4N were observed in 70.5 ± 2.2% and 66.9 ± 4.5% of $p53^{-/-}$ MEFs after 22 hours of exposure to nocodazole or colcemid, respectively, whereas only 22 ± 1.9% and 22.1 ± 0.3% of $p53^{+/+}$ MEFs developed DNA contents greater than 4N under the same conditions. DNA contents greater than 8N were observed in 49.8% and 48.5% of $p53^{-/-}$ cells after 44 hours of exposure to nocodazole or colcemid, respectively, compared with 0% of $p53^{+/+}$ cells. There was no evidence of aggregation artifacts that could lead to tetraploid and octaploid DNA contents, and the results were reproduced by flow cytometric protocols with the use of three different DNA dyes [4,6-diamidino-2-phenylindole (DAPI), propidium iodide, and Hoechst 33342].

Cycling tetraploid and octaploid cell populations were not observed in $p53^{-/-}$ MEFs after exposure to mimosine, a G_1 inhibitor, or to either aphidicolin or hydroxyurea, which are S phase inhibitors; less than 10% of $p53^{-/-}$ MEFs had DNA contents greater than 4N after a 22-hour exposure and none had DNA contents greater than 8N after 44 hours. The $p53^{-/-}$ MEFs that were exposed to VM26, a G_2 inhibitor, developed a small tetraploid S phase (15.2 ± 1.2% of cells had DNA contents greater than 4N after 22 hours), whereas $p53^{+/+}$ MEFs did not. The $p53^{-/-}$ cells exposed to VM26 did not develop cycling octaploid cell populations. Cytoge-

S. M. Cross, C. A. Sanchez, C. A. Morgan, M. K. Schimke, W. H. Raskind, B. J. Reid, Department of Medicine, University of Washington, Seattle, WA 98195, USA.
S. Ramel, Department of Surgery, Ersta Hospital, S-116 35 Stockholm, Sweden.
R. L. Idzerda, Department of Pharmacology, University of Washington, Seattle, WA 98195, USA.
*To whom correspondence should be addressed.

netic analysis confirmed the development of tetraploid and octaploid metaphases in $p53^{-/-}$ MEFs (Fig. 2). In two experiments, after 22 hours in nocodazole a mean of 46.5% of $p53^{-/-}$ metaphase cells were tetraploid and 13.5% were octaploid, whereas only 18% of $p53^{+/+}$ metaphase cells were tetraploid and none were octaploid.

Taken together, these results indicate that p53 is a component of a spindle checkpoint in mouse cells in culture. They also suggest that there is a baseline requirement for this checkpoint during cell division even in the absence of spindle inhibitors because 50% of $p53^{-/-}$ MEFs became tetraploid by passage 7, which is consistent with data reported by other investigators (*7*, *12*).

We next studied genetically modified mice to see if p53 deficiency or inactivation of p53 protein by SV40 T antigen predisposed them to the development of tetraploid cell populations in vivo. Pancreatic samples from three control mouse strains had normal 4N fractions (≤7%), with no evidence of tetraploid S phase fractions or octaploid cell populations (Fig. 3A). However, pancreatic samples from $p53^{-/-}$ mice

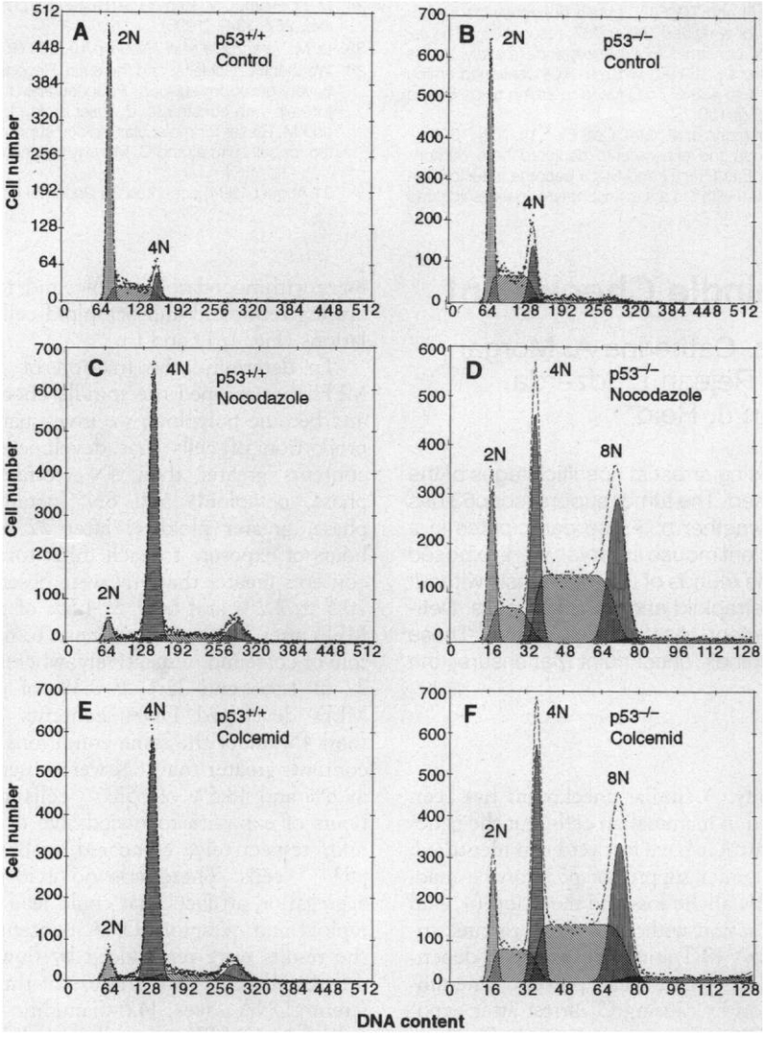

Fig. 1. DNA content flow cytometric histograms of $p53^{-/-}$ and $p53^{+/+}$ MEFs. All experiments were performed on MEFs between passages 1 and 3. MEFs were prepared by a method modified from (*12*). MEFs were grown in 25-cm^3 flasks in Dulbecco's modified Eagle's medium (DMEM; Gibco) with 20% fetal calf serum (FCS) (Hyclone, Logan, Utah), penicillin (10 U/ml; Gibco), and streptomycin (10 μg/ml; Gibco) and transferred at first passage to six-well (35-mm) cluster plates (Costar, Pleasanton, California) at approximately 7×10^4 cells per well. Doubling times of the $p53^{-/-}$ and $p53^{+/+}$ MEFs were 19.9 ± 2.9 and 18.4 ± 1.9 hours, respectively. Nocodazole (Sigma) (0.12 μg/ml) and colcemid (Sigma) (0.50 μg/ml) were added to logarithmically growing cells, and cells with and without the added inhibitor were incubated for 22 (shown) and 44 hours. DNA content flow cytometry was performed as described (*9*, *21*). The development of tetraploid and octaploid cell populations was confirmed for nocodazole and colcemid in five and three different experiments, respectively. (**A**) Untreated $p53^{+/+}$ MEFs. (**B**) Untreated $p53^{-/-}$ MEFs. Less than 10% of early passage MEFs are tetraploid. (**C**) $p53^{+/+}$ MEFs in nocodazole. (**D**) $p53^{-/-}$ MEFs in nocodazole. There is a tetraploid cell population with a tetraploid S phase fraction and a large 8N fraction. Bromodeoxyuridine (BrdU)-DNA content multiparameter flow cytometry confirmed that the tetraploid S phase cells incorporated BrdU. (**E**) $p53^{+/+}$ MEFs in colcemid. (**F**) $p53^{-/-}$ MEFs in colcemid. The shading is the visual representation of the computer-generated quantification of the data. Primary data are shown as dots, and the computer best fit of the data is shown as a dashed line. The numbers on the *x* axis represent flow cytometric channel units. Actual DNA contents of the cells are indicated in the figures.

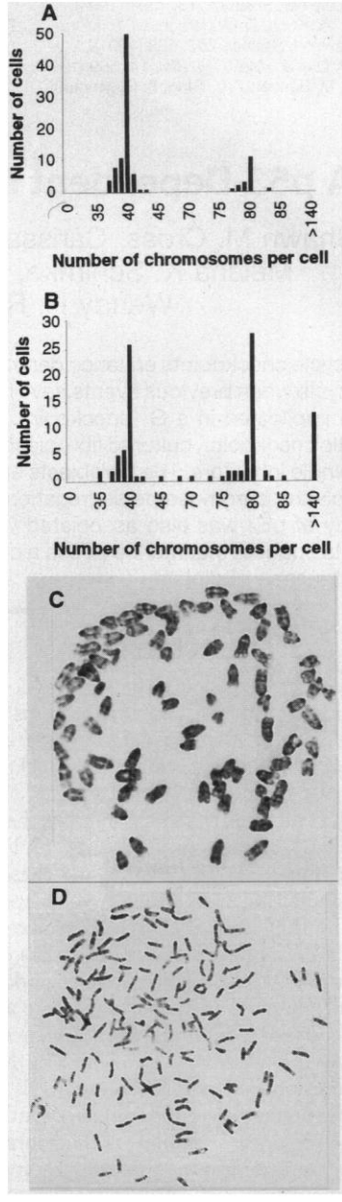

Fig. 2. Cytogenetic analysis of MEFs after exposure to nocodazole. Both $p53^{+/+}$ (**A**) and $p53^{-/-}$ (**B**) MEFs were prepared as in Fig. 1 and exposed to nocodazole for 22 hours. Cytogenetic analysis was performed as in (*22*). Similar results were observed in two separate experiments. (**C**) $p53^{-/-}$ tetraploid metaphase cell. (**D**) $p53^{-/-}$ metaphase cell with ~160 chromosomes.

developed a cycling tetraploid cell population that increased steadily from day 8 through day 24, at which time up to 28% of the cells were tetraploid. A cycling tetraploid cell population also developed in the pancreases of elastase-SV40 T antigen transgenic mice between 18 and 24 days after birth (Fig. 3A) (*8, 9*). The development of tetraploid cell populations was confirmed by cytogenetic analysis (Fig. 3B). Thus, loss of p53 function is associated with the development of tetraploidy in vivo as well as in vitro.

To determine whether $p53^{-/-}$ cells are deficient in a spindle assembly checkpoint that leads to metaphase arrest after exposure to spindle inhibitors, we investigated the mitotic index of $p53^{+/+}$ and $p53^{-/-}$ MEFs in the presence and absence of nocodazole. After exposure to nocodazole, $p53^{+/+}$ MEFs showed a mitotic delay with an initial increase in the proportion of cells with condensed chromosomes, followed by a decrease after 6 hours (Fig. 4). The $p53^{-/-}$ MEFs had a smaller increase in mitotic index than did $p53^{+/+}$ MEFs. When $p53^{+/+}$ or $p53^{-/-}$ MEFs were exposed simultaneously to nocodazole and either of the S phase inhibitors aphidicolin or hydroxyurea, there was an initial small increase in mitotic index followed by a decline that appeared somewhat more rapid in the $p53^{-/-}$ cells. Combined with other data (Figs. 1 and 2), these results suggest that $p53^{-/-}$ MEFs have a decreased mitotic delay after exposure to spindle inhibitors and are also deficient in a control that prevents two successive S phases in cells that have not correctly completed an intervening mitosis.

Our results suggest a similarity between $p53^{-/-}$ mouse cells and *bub* and *mad* mutants of *S. cerevisiae* (*3*). The genes encoding BUB and MAD are part of a surveillance system that monitors the integrity of the spindle and that may enhance genetic fidelity by delaying cell cycle progression when spindle function is lost or when chromosomes lag in their attachment to the mitotic apparatus (*3, 13*). The apparently spontaneous development of tetraploid cell populations that we observed in $p53^{-/-}$ mouse cells suggests a requirement for this checkpoint during normal cell division even in the absence of spindle inhibitors.

The $p53^{+/+}$ cells appear to adapt after exposure to nocodazole, leading to chromosome decondensation and the morphology of interphase nuclei. Although most $p53^{+/+}$ MEFs are prevented from entering the S phase prematurely after exposure to spindle inhibitors, some continue cell cycle progression and form cycling tetraploid cells, which is consistent with previous observations (*14*). In addition, the metaphase delay induced by exposure to spindle inhibitors is decreased in $p53^{-/-}$ MEFs, and $p53^{-/-}$ MEFs can reenter the S phase prematurely in the presence of these inhibitors. The spindle assembly checkpoint may be more stringent in human than in rodent cells, but this conclusion is based on experiments with cell lines containing multiple genetic abnormalities (*15, 16*).

It is possible that human cells have evolved different or additional controls for the p53-dependent spindle checkpoint because some human cell lines that lack functional p53 because of papilloma virus E6 or SV40 T antigen expression arrest after exposure to spindle inhibitors (*15, 16*). However, SV40-infected human diploid fibroblasts and other human cell lines, including fibroblasts from patients with ataxia telangiectasia, become polyploid spontaneously or after treatment with spindle inhibitors (*16, 17*). Furthermore, a recent study reported that p53 overexpression was associated with the transition from diploidy to tetraploidy in human colon cancer, and the authors suggested that inactivation of p53 might lead to endoreduplication in vivo (*11*).

Tetraploid cell populations have been observed in a large number of human and rodent solid tissue neoplasms (*18*). This has led to the hypothesis that tetraploid cells are unstable intermediates that are predisposed to the development of aneuploidy during neoplastic progression (*19*). Support for this hypothesis comes from studies of elastase-SV40 T antigen transgenic mice in which T antigen expression and p53 inactivation are followed by the development of

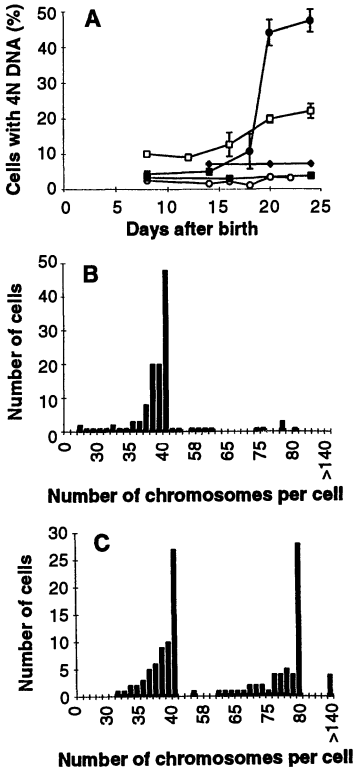

Fig. 3. (**A**) 4N DNA content (G_2, tetraploid) fractions in pancreatic samples from elastase-SV40 T antigen transgenic mice (closed circles), $p53^{-/-}$ mice (open squares), $p53^{+/+}$ control mice from the same litter (closed diamonds), 129 SVJ control mice (closed squares), and BGSjLE1 control mice (open circles). Two to five mice were studied at each time point. Transgenic mice homozygous for the elastase-SV40 T antigen [transgenic mouse line 264-4; Tg(E1a-1,SV40E+E1a-1,neo)Bril9] gene (*8, 9*) were studied. Mice that are heterozygous (+/−) and homozygous deficient (−/−) for p53 are described in (*23*). Heterozygous females were mated with heterozygous or homozygous p53-deficient males to produce mice that were $p53^{+/+}$ and $p53^{-/-}$. Three p53 wild-type control strains were evaluated, including $p53^{+/+}$ mice from the same litter, 129 SVJ mice, and BGSjLE1 mice (Jackson Laboratory, Bar Harbor, Maine). Mice were killed (2 to 4 min in a dry ice chamber) and dissected promptly in accordance with the policies established by the Animal Care Committee of the University of Washington. Pancreatic tissue was dissected and placed in modified Eagle's medium with 10% dimethyl sulf- oxide and 5% fetal calf serum and frozen at −70°C until processed for flow cytometric evaluation as in (*9*). (**B** and **C**) Cytogenetic analysis of pancreatic samples from elastase-SV40 T antigen transgenic mice. Pancreatic tissue was obtained from one male and one female at 14 (B) or 22 (C) days after birth and prepared for cytogenetic analysis as in (*22*). An average of 143 metaphase cells was evaluated for each mouse.

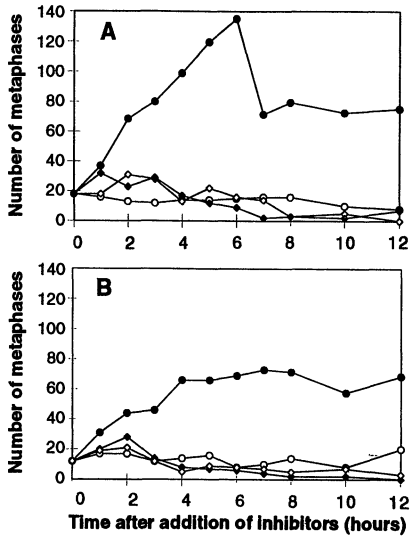

Fig. 4. Kinetics of appearance of diploid metaphase cells in control and nocodazole-treated MEFs. We prepared $p53^{+/+}$ (**A**) and $p53^{-/-}$ (**B**) MEFs as in Fig. 1. At time 0, exponentially growing $p53^{+/+}$ and $p53^{-/-}$ MEFs were divided into untreated control cultures (open circles) or cultures exposed to nocodazole (0.12 μg/ml) (closed circles), nocodazole and hydroxyurea (open diamonds), or nocodazole and aphidicolin (closed diamonds). Samples were taken at 1-hour intervals and evaluated cytogenetically as in Fig. 2. The *y* axis indicates the number of metaphase cells per 1000 cells.

tetraploid and then multiple aneuploid cell populations (*8*, *20*). We have shown previously that formation of tetraploid pancreatic cells in these mice coincides with the appearance of cells displaying multiple centrioles and undergoing multipolar mitoses (*9*). These results suggest a mechanism for the development of a genetically unstable tetraploid cell population during neoplastic progression. Mouse cells devoid of the p53-dependent spindle checkpoint are capable of completing events of the subsequent cell cycle, including DNA synthesis, without completing chromosome segregation. Replication of DNA and reduplication of centrosomes and centrioles without completion of chromosome segregation in mitosis could lead to the formation of a tetraploid cell that has an abnormal number of mitotic poles, predisposing the organism to multipolar mitoses, chromosome segregation abnormalities, aneuploidy, and cancer.

REFERENCES AND NOTES

1. L. H. Hartwell and D. Smith, *Genetics* **110**, 381 (1985).
2. M. Brown *et al.*, *Cold Spring Harbor Symp. Quant. Biol.* **56**, 359 (1991); A. W. Murray, *ibid.*, p. 399; T. A. Weinert and L. H. Hartwell, *Science* **241**, 317 (1988); M. Dasso and J. W. Newport, *Cell* **61**, 811 (1990); T. Enoch and P. Nurse, *ibid.* **60**, 665 (1990); L. H. Hartwell and T. A. Weinert, *Science* **246**, 629 (1989); L. H. Hartwell, J. Culotti, J. R. Pringle, B. J. Reid, *ibid.* **183**, 46 (1974); D. Broek, R. Bartlett, K. Crawford, P. Nurse, *Nature* **349**, 388 (1991).
3. R. Li and A. Murray, *Cell* **66**, 519 (1991); M. A. Hoyt, L. Totis, B. T. Roberts, *ibid.*, p. 507.
4. S. J. Baker *et al.*, *Science* **244**, 217 (1989); M. Hollstein, D. Sidransky, B. Vogelstein, C. C. Harris, *ibid.* **253**, 49 (1991).
5. D. P. Lane and L. V. Crawford, *Nature* **278**, 261 (1979); D. I. H. Linzer and A. J. Levine, *Cell* **17**, 43 (1979); A. J. Levine, J. Momand, C. A. Finlay, *Nature* **351**, 453 (1991).
6. M. B. Kastan, O. Onyekwere, D. Sidransky, B. Vogelstein, R. W. Craig, *Cancer Res.* **51**, 6304 (1991); S. J. Kuerbitz, B. S. Plunkett, W. V. Walsh, M. B. Kastan, *Proc. Natl. Acad. Sci. U.S.A.* **89**, 7491 (1992); M. B. Kastan *et al.*, *Cell* **71**, 587 (1992); Y. Yin, M. A. Tainsky, F. Z. Bischoff, L. C. Strong, G. M. Wahl, *ibid.* **70**, 937 (1992); X. Lu and D. P. Lane, *ibid.* **75**, 765 (1993).
7. L. R. Livingstone *et al.*, *Cell* **70**, 923 (1992).
8. D. M. Ornitz, R. E. Hammer, A. Messing, R. D. Palmiter, R. L. Brinster, *Science* **238**, 188 (1987).
9. D. S. Levine, C. A. Sanchez, P. S. Rabinovitch, B. J. Reid, *Proc. Natl. Acad. Sci. U.S.A.* **88**, 6427 (1991).
10. G. J. A. Offerhaus *et al.*, *Gastroenterology* **102**, 1612 (1992); P. L. Blount *et al.*, *Cancer Res.* **54**, 2292 (1994); K. Neshat *et al.*, *Gastroenterology* **106**, 1589 (1994).
11. P. Carder *et al.*, *Oncogene* **8**, 1397 (1993).
12. M. Harvey *et al.*, *ibid.*, p. 2457.
13. R. E. Zirkle, *Radiat. Res.* **41**, 516 (1970); C. L. Reider and S. P. Alexander, in *Mechanisms of Chromosome Distribution and Aneuploidy*, M. Resnick and B. Vig, Eds. (Liss, New York, 1989), pp. 185–194.
14. H. N. Barber and H. G. Callan, *Proc. R. Soc. London Ser. B.* **131**, 258 (1942); R. J. Wang and L. Yin, *Exp. Cell Res.* **101**, 331 (1976).
15. A. L. Kung, S. W. Sherwood, R. T. Schimke, *Proc. Natl. Acad. Sci. U.S.A.* **87**, 9553 (1990).
16. R. T. Schimke, A. L. Kung, D. F. Rush, S. W. Sherwood, *Cold Spring Harbor Symp. Quant. Biol.* **56**, 417 (1991).
17. N. M. Lopes, E. G. Adams, T. W. Pitts, B. K. Bhuyan, *Cancer Chemother. Pharmacol.* **32**, 235 (1993); J. Liebmann *et al.*, *ibid.* **33**, 331 (1994); J. R. Roberts, D. C. Allison, R. C. Donehower, E. K. Rowinsky, *Cancer Res.* **50**, 710 (1990); J. Laffin, D. Fogleman, J. M. Lehman, *Cytometry* **10**, 205 (1989); S. G. Kuhar and J. M. Lehman, *Oncogene* **6**, 1499 (1991).
18. A. Levan, *Ann. N.Y. Acad. Sci.* **63**, 774 (1956); J. A. Kirkland, M. A. Stanley, K. M. Cellier, *Cancer* **20**, 1934 (1967); P. A. Bunn, S. Kransnow, R. W. Makuch, M. L. Schlam, G. P. Schlechter, *Blood* **59**, 528 (1982); A. Jakobsen, S. Mommsen, S. Olsen, *Cytometry* **4**, 170 (1983); H. Wijkstrom, I. Granberg-Ohman, B. Tribukait, *Cancer* **53**, 1718 (1984); J. R. Shapiro and W. R. Shapiro, *Cancer Metastasis Rev.* **4**, 107 (1985); W. T. Knoefel, U. Otto, H. Baisch, G. Kloppel, *Cancer Res.* **47**, 221 (1987); D. R. Burholt *et al.*, *ibid.* **49**, 3355 (1989).
19. S. E. Shackney *et al.*, *Cancer Res.* **49**, 3344 (1989).
20. S. Ramel *et al.*, *Pancreas*, in press.
21. D. J. Arndt-Jovin and T. M. Jovin, *J. Histochem. Cytochem.* **25**, 585 (1977); J. Gong, B. Ardelt, F. Traganos, Z. Darzynkiewicz, *Cancer Res.* **54**, 4285 (1994).
22. W. H. Raskind *et al.*, *Cancer Res.* **52**, 2946 (1992).
23. T. Jacks *et al.*, *Curr. Biol.* **4**, 1 (1994).

24. We thank L. Hartwell and T. Jacks for thoughtful discussions and critical review of this manuscript; D. Cowan, R. Sudore, P. Galipeau, and the University of Washington flow cytometry core facility for technical assistance; R. Brinster and E. Sandgren for the Tg264-4 transgenic mice; and T. Jacks for p53-deficient mice. Supported by NIH grant R01CA55814, American Cancer Society grant EDT-21E, the Ryan Hill Research Foundation, and the Ersta Hospital Research Fund.

30 August 1994; accepted 9 January 1995

Impact of CLOD Pathogen on Pacific Coral Reefs

Mark M. Littler and Diane S. Littler

A bacterial pathogen of coralline algae was initially observed during June 1993 and now occurs in South Pacific reefs that span a geographic range of at least 6000 kilometers. The occurrence of the coralline algal pathogen at Great Astrolabe Reef sites (Fiji) increased from zero percent in 1992 to 100 percent in 1993, which indicates that the pathogen may be in an early stage of virulence and dispersal. Because of the important role played by coralline algae in reef building, this pathogen, designated coralline lethal orange disease (CLOD), has the potential to greatly influence coral reef ecology and reef-building processes.

Barrier, fringing, and atoll reefs are complex ecosystems that depend on calcareous coralline algae for the maintenance of wave-resistant fronts. Crustose coralline algae (an order of the Rhodophyta or red algal phylum) are plants that deposit a particularly hard and geologically resistant form of calcium carbonate (calcite). These algae cement together much of the sand, dead coral, and debris to create a stable substrate. Many have a prostrate-type growth form and look like red, pink, or purple cement covering large areas of the reef, whereas others form upright branched heads much like the corals. Crustose coralline algae, particularly *Porolithon onkodes* in the Pacific and *Porolithon pachydermum* in the Atlantic, are the principal cementing agents that produce the structural integrity and resilience of the outer reef rim. Coralline algae are important for the absorption of wave energy that would otherwise erode shoreward land masses and for the facilitation of the development of most other shallow reef communities (*1*, *2*).

No previously characterized diseases cause significant mortality of coralline algae. However, diseases resulting in bandlike tissue necrosis and colony death are known for western Atlantic (*3*) and Great Barrier Reef (*4*) reef-building corals. The variety of microorganisms reported in association with necrotic bands on corals include the cyanobacterium *Phormidium corallyticum* [shown to cause black band disease (*5*)] and the bacteria *Beggiatoa* and *Desulfovibrio* [present secondarily (*6*)]. Most ecological studies of algal pathogens have concentrated on freshwater phytoplankton or benthic diatoms; few data exist on the importance of pathogens in marine macroalgae and no pathogens are known for coralline algae.

Here we describe the growth habit of a bright orange bacterial pathogen that is lethal to coralline algae (termed coralline lethal orange disease, CLOD). CLOD is similar to the coral banding diseases in that the pathogen occurs as a line or front that moves across the host and leaves completely dead skeletal carbonate behind. Because of the critical role played by coralline algae in forming reef rims throughout the Indo-Pacific (*2*) and because reef-building coralline algae extend to much greater latitudes and depths than hermatypic corals (*7*), CLOD may influence reef ecology and reef-building processes.

Coralline lethal orange disease was initially recorded on southwest Aitutaki Island, Cook Islands (Fig. 1), from the back reef through the barrier reef algal ridge and throughout the fore-reef spur and groove to a depth of 30 m (*8*). The pathogen appeared as conspicuous bright orange dots that spread to become thin circular rings (up to

Department of Botany, National Museum of Natural History, Smithsonian Institution, Washington, DC 20560, USA.